DISCLAIMER

This contractor document was prepared for the U.S. Department of Energy (DOE), but has not undergone programmatic, policy, or publication review, and is provided for information only. The document provides preliminary information that may change based on new information or analysis, and represents a conservative treatment of parameters and assumptions to be used specifically for Total System Performance Assessment analyses. The document is a preliminary lower level contractor document and is not intended for publication or wide distribution.

Although this document has undergone technical reviews at the contractor organization, it has not undergone a DOE policy review. Therefore, the views and opinions of authors expressed may not state or reflect those of the DOE. However, in the interest of the rapid transfer of information, we are providing this document for your information per your request.

NM3507

OFFICE OF CIVILIAN RADIOACTIVE WASTE MANAGEMENT
ANALYSIS/MODEL COVER SHEET

1. QA: QA

Page: 1 of: 29

Complete Only Applicable Items

2. ☒ Analysis — Check all that apply

Type of Analysis	☐ Engineering ☐ Performance Assessment ☒ Scientific
Intended Use of Analysis	☐ Input to Calculation ☒ Input to another Analysis or Model ☐ Input to Technical Document
Describe use: Support for Waste form PMR	

3. ☐ Model — Check all that apply

Type of Model	☐ Conceptual Model ☐ Abstraction Model ☐ Mathematical Model ☐ System Model ☐ Process Model
Intended Use of Model	☐ Input to Calculation ☐ Input to another Model or Analysis ☐ Input to Technical Document
Describe use:	

4. Title:
Hydride-Related Degradation of SNF Cladding under Repository Conditions

5. Document Identifier (including Rev. No. and Change No., if applicable):
ANL-EBS-MD-000011 REV 00

6. Total Attachments:
N/A

7. Attachment Numbers - No. of Pages in Each:
N/A

	Printed Name	Signature	Date
8. Originator	Hee Chung	Hee Chung	3-3-00
9. Checker	Michael Bale	Michael E. Bale	3-6-00
10. Lead/Supervisor	Christine Stockman	Christine Stockman	3-6-00
11. Responsible Manager	David Stahl	David Stahl	3/7/00

12. Remarks:

INFORMATION COPY

LAS VEGAS DOCUMENT CONTROL

OFFICE OF CIVILIAN RADIOACTIVE WASTE MANAGEMENT
ANALYSIS/MODEL REVISION RECORD

Complete Only Applicable Items

2. Analysis or Model Title:

Hydride-Related Degradation of SNF Cladding under Repository Conditions

3. Document Identifier (including Rev. No. and Change No., if applicable):

ANL-EBS-MD-000011

4. Revision/Change No.	5. Description of Revision/Change
REV 00	Initial Issue

CONTENTS

CONTENTS (Continued)

Page

FIGURES

Page

TABLES

Page

ACRONYMS AND ABBREVIATIONS

BWR	boiling water reactor
CANDU	Canada Deuterium Uranium Reactor
CSNF	commercial spent nuclear fuel
DBT	ductile brittle transition
DHC	delayed hydride cracking
ID	inner diameter
LWR	light water reactor
OD	outer diameter
PWR	pressurized water reactor
QA	Quality Assurance
RAH	radiation anneal hardening
SNF	spent nuclear fuel

1. PURPOSE

The objective of this study is to analyze the degradation of commercial spent nuclear fuel (CSNF) cladding under repository conditions by the hydride-related metallurgical processes, such as delayed hydride cracking (DHC), hydride reorientation and hydrogen embrittlement, thereby, providing a better understanding of the degradation process and clarifying which aspects of the process are known and which need further evaluation and investigation.

This report was developed in accordance with the development plan, *Waste Package Materials Department Analysis and Modeling Reports Supporting the Waste Form PMR* (CRWMS M&O 2000a). The scope of this AMR is outlined in the section entitled, "Hydride-Related Degradation of SNF Cladding under Repository Conditions," of that development plan.

2. QUALITY ASSURANCE

The Quality Assurance (QA) program applies to this analysis. All types of waste packages were classified (per QAP-2-3 REV 10) as Quality Level-1 in *Classification of the MGR Uncanistered Spent Nuclear Fuel Disposal Container System* (CRWMS M&O 1999a, p. 7). This analysis applies to all of the waste package designs included in the MGR Classification Analyses. Reference CRWMS M&O (1999a) is cited as an example. The development of this analysis is conducted under activity evaluation *1101213FM3 Waste Form Analyses & Models - PMR* (CRWMS M&O 1999b), which was prepared per QAP-2-0 REV 5. The results of that evaluation were that the activity is subject to the *Quality Assurance Requirements and Description* (DOE 2000) requirements.

3. COMPUTER SOFTWARE AND MODEL USAGE

No computer software subject to the requirements of the Quality Assurance Requirements Document (QARD) was used in this report. No models were used in this report.

4. INPUTS

Inputs and their sources have been identified, documented, and referenced in the pertinent sections or subsections in accordance with AP-3.15Q Procedure.

4.1 DATA AND PARAMETERS

Data that are used directly to reach the conclusions of this report are listed in Table 1. These data are from several papers published in open literature identified in the table.

Table 1. List of Data that are Directly Used to Reach the Conclusions

Data	Description	Source	Used in
≈5.5 MPa $m^{1/2}$	Minimum of critical stress intensities reported for crack propagation by delayed hydride cracking process under isothermal conditions; the range of data reported in the source papers is ≈5.5 to ≈8 MPa $m^{1/2}$	Simpson and Puls 1979 Puls et al. 1982 Davies and Stearns 1986 Shih and Puls 1996	Section 6.3.5
≈143 MPa	Applied internal stress under which hydride reoriented spent PWR cladding (burnup ≈30 MWd/kgU) remained intact during slow cooling to room temperature after exposure to ≈323°C for ≈87 days	Einziger and Kohli 1984	Section 6.4.2

4.2 CRITERIA

No specific criteria have been used in this report.

4.3 CODES AND STANDARDS

No codes or standards have been used in this report.

5. ASSUMPTIONS

No specific assumptions have been made or used in this report that directly influence the results of the analysis.

6. ANALYSIS/MODEL

6.1 BACKGROUND

In spent nuclear fuel (SNF) rods discharged from commercial nuclear reactors, cladding is a distinct structural barrier that prevents or limits the release of radionuclides from the fuel, therefore long-term structural integrity of the cladding has been identified as one of the key factors that influence the overall performance of a repository system (CRWMS M&O 2000b).

The cladding of fuel rods from most commercial nuclear reactors in the U.S. is fabricated from Zr-based alloys, i.e., Zircaloy-2 in boiling water reactor (BWR) fuel and Zircaloy-4 in pressurized water reactor (PWR) fuel. After typical fuel burnup that ranges from ≈25 to ≈60 MWd/kgU in a reactor, the microstructure of the Zircaloy cladding is significantly modified as a result of ≈3-5 years of exposure to severe conditions in a reactor, i.e., high-temperature, corrosion, errosion, irradiation, and stress. The microstructure of a CSNF cladding is usually characterized by dense irradiation damages, waterside oxide layer (thickness ranging from ≈15 to ≈100 μm), hydrides, increased concentration of oxygen and hydrogen solutes in the clad, and for some high-burnup fuel cladding, a tight layer bonded between pellet and cladding. Therefore, the structure and properties of CSNF cladding differ significantly from those of fresh nonirradiated cladding.

As a consequence of decay heat production, CSNF cladding placed in the proposed Yucca Mountain repository is projected to be initially heated and then undergoes a time-temperature excursion similar to that shown in Figure 1. Note that peak cladding temperature at ≈10-20 years after closure is not well quantified, because it is a significant function of the design of the repository. Initially, fuel cladding is projected to be exposed to an inert atmosphere that fills the waste package (e.g., helium gas); then the cladding temperature falls < 100°C. At some stage, the waste package could be breached, and water could penetrate the package subsequently. Several reviews of the behavior of CSNF cladding under long-term repository conditions have been reported (Rothman 1984; Pescatore et al. 1990; CRWMS M&O 1998; S. Cohen & Associates 1999; Henningson 1998). Among the many factors and parameters of the repository, peak cladding temperature is the most important parameter in influencing the cladding performance. CRWMS M&O (1998) estimated that the peak cladding temperature for the design-basis waste package of the Yucca Mountain repository will be ≈325°C, although the average temperature of the cladding was estimated to be < 240°C.

Although large uncertainties persist, hydride-related metallurgical processes have been identified as possible degradation mechanisms that can potentially compromise the structural integrity of cladding. The hydride-related degradation of Zircaloy cladding can be classified into two distinct processes, i.e., DHC and hydride reorientation followed by potential stress-rupture failure. Considering the repository environment and the projected time-temperature history of cladding, gross embrittlement by excessive hydrogen uptake and virtual conversion of the cladding wall to hydride is extremely unlikely.

Hydrogen uptake and hydriding are more significant in PWR fuel cladding than in BWR fuel cladding, because the former is exposed to a high hydrogen overpressure at a higher temperature (i.e., ≈325°C vs. ≈289°C) and because the oxide layer in a PWR fuel cladding tends to develop

microcracks and pores as burnup is increased, leading to a higher rate of permeation of hydrogen. Therefore, the present analysis and modeling will be focused as a bounding case on hydride-related degradation of Zircaloy-4 clad PWR SNF cladding.

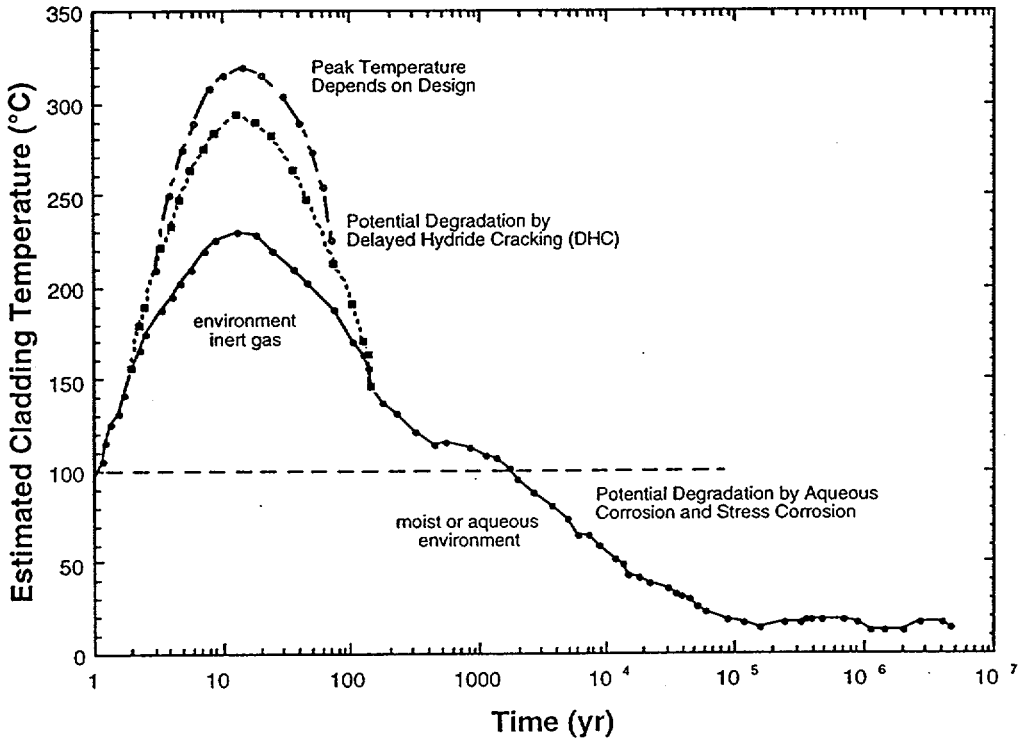

Figure 1. Estimated CSNF Cladding Temperature versus Time after Repository Closure and Possible Cladding Degradation Mechanisms

6.2 STRUCTURE AND CHARACTERISTICS OF CSNF CLADDING

The cladding temperature in most operating PWRs is ≈315 to ≈325°C. The average hydrogen concentration in the cladding could increase from < 20 ppm by weight (wppm) at zero fuel burnup to as much as ≈800 wppm at ≈60 MWd/kgU. The degree of hydrogen uptake and hydriding is influenced by many factors, such as cladding temperature, fuel burnup, cladding fluence, cladding alloy composition, fabrication history, texture, and, most of all, the degree of oxidation (e.g., thickness of coolant-side oxide layer). As an approximation, ≈12-18% of all hydrogen atoms generated from the process of the cladding oxidation is picked up by the cladding in a PWR (Garde 1989).

Most data base and understanding available in the literature on DHC and hydride reorientation are based on the results of investigations on either unirradiated Zr alloys (i.e., Zr, Zircaloy-2, Zircaloy-4, and Zr-2.5%Nb) in the laboratory or irradiated Zr-2.5%Nb Canadian Deuterium Uranium (CANDU) reactor pressure tubes in hot cells. However, the texture, microstructure, and mechanical properties of such laboratory test specimens or CANDU pressure tubes are not the same as those of CSNF cladding. Therefore, before an attempt is made to analyze hydride-related degradation in CSNF cladding under repository conditions, it is necessary to review

important metallurgical characteristics of CSNF cladding and the loading patterns expected under repository conditions.

6.2.1 Phase Structure

In unirradiated state, the concentration of the alloying elements in standard Zircaloy-4 cladding is approximately (in wt.%) 1.5 Sn, 0.2 Fe, 0.01 Ni, and 0.1 Cr. It also contains hydrogen < 20 wppm and oxygen 0.10-0.12 wt.%. Neither hydrides nor oxides are present inside the material in fresh unirradiated state. The solubility of Fe, Ni, and Cr in Zr-base alloys is, however, very low. Therefore, most Fe, Ni, and Cr atoms in nonirradiated Zr alloys at ≈300°C exist either in a metastable state as solute atoms or as $Zr(Cr,Fe)_2$ or $Zr_2(Ni,Fe)$ precipitates in Zircaloys. This indicates that Fe plays a central role in forming thermal precipitates. Annealing at higher temperatures for longer periods increases the size and volume fraction of $Zr(Cr,Fe)_2$ or $Zr_2(Ni,Fe)$ precipitates in Zircaloys. This in turn leads to a lower concentration of these solutes in the matrix and, hence, to a higher corrosion rate. Effects of fabrication variables on precipitate size and distribution have been, therefore, investigated extensively. For in-reactor corrosion, however, the situation is more complicated because $Zr(Cr,Fe)_2$ and $Zr_2(Ni,Fe)$ precipitates become amorphous gradually under irradiation, and as a consequence, Fe, Cr, and Ni atoms are slowly released into the alloy matrix.

6.2.2 Texture

The basal pole of CSNF cladding is predominantly aligned ≈30° away from the radial direction of the tubing. This texture is primarily determined by the tube fabrication process, especially by the ratio of tube-diametral reduction to wall-thickness reduction. Although second-phase precipitates become amorphous and dissolved back to grain matrices as the neutron fluence is increased, the texture of the cladding tube is not altered by irradiation. The characteristic texture has large effects on the hydride structure of CSNF cladding, because the habit plane of hydride precipitation is very close to the basal plane of the cladding (see below). As a result, hydride platelets in CSNF cladding are oriented predominantly in the circumferential direction. In this direction, hydride platelets are not deleterious to cladding mechanical properties under typical stress in a PWR in which tension in the tangential direction is the primary stress.

6.2.3 Oxidation and Oxide Layer

The oxidation behavior of Zircaloys is characterized by a transition from cubic, to parabolic, and to linear breakaway oxidation as fuel burnup increases, either in the form of localized nodular oxidation in Zircaloy-2 in BWRs or uniform breakaway oxidation in Zircaloy-4 in PWRs. For example, after the onset of breakaway oxidation which is influenced strongly by decrease in thermal conduction and increase in metal temperature, oxide layer thickness in the upper grid spans of standard Zircaloy-4 fuel cladding (concentration of Sn ≈1.5 wt.%) increases almost exponentially at burnups higher than ≈50 MWd/kgU. As an extreme case, an oxide layer as thick as ≈100 μm can be produced in standard Zircaloy-4 cladding at a peak rod burnup of ≈60 MWd/kgU. However, the oxide layer thickness in most PWR cladding is expected to range from ≈15 to ≈80 μm. The onset and rate of breakaway oxidation of standard Zircaloy-4 cladding in PWRs are sensitive to operational conditions such as local cladding temperature under

irradiation, water chemistry, grid span position, and to cladding microchemistry and fabrication procedure.

In the breakaway oxidation regime, oxide morphology changes from a compact adherent black layer to a porous, flaky, grayish-white layer (see Fig. 2). The latter morphology allows more rapid migration of oxygen and permeation of hydrogen from the reactor coolant side to metal cladding. Breakaway oxidation is the primary cause of reduced metal thickness, enhanced hydrogen uptake and hydriding, and high levels of oxygen in solution in the load-bearing metallic phase of the cladding. Cladding mechanical properties could degrade significantly if these processes are excessive.

The microstructure near the metal/oxide boundary in pre- and post-breakaway oxidation stages is characterized by different mixtures of zirconium suboxides (metal side), tetragonal ZrO_2, and monoclinic ZrO_2 (coolant side). Stabilization of tetragonal ZrO_2 at the metal/oxide boundary suppresses breakaway oxidation, which may be related to a higher fracture toughness of tetragonal ZrO_2 compared to that of monoclinic modification of ZrO_2. A noncracked layer of this innermost oxide (denoted as L_{OX} in Fig. 2) is always present between the metal and the outer porous oxide in irradiated PWR cladding. Therefore, no bare metal will be exposed to the surrounding environment, unless a fully penetrating radial crack is produced in the oxide layer.

6.2.4 Irradiation Damage

Irradiation damage is a loosely defined term commonly used to describe general microstructural features associated with irradiation of one type or another. Damage in neutron-irradiated Zircaloy-4 under LWR operating conditions is in the form of vacancies, interstitials, "black-dot" defects (clusters of irradiation-induced defects), small dislocation loops, short line dislocations, and dislocation entanglements.

The nature and number density of irradiation-induced damage are strongly influenced by irradiation temperature, neutron flux, fluence, alloying elements, minor impurities, coldwork, and other fabrication variables of the cladding. Mechanical properties of CSNF cladding is strongly influenced by irradiation temperature and damage; therefore, great caution must be exercised when data from test reactors are interpreted and the applicability of such data relative to the behavior of CSNF cladding is evaluated.

Dislocation loops and short line dislocations in Zircaloy irradiated to low fluence in LWR or CANDU reactors at ≈300°C are mainly <a>-type, meaning that the associated Burgers vector has an <a>-component of the hexagonal close-packed (hcp) unit cell of the α-phase Zircaloy. This is related to the <a>-component Burgers vector of the prism slip system of the hcp structure, which is the only slip system in α-phase Zircaloy under tension in as-fabricated state. However, as fluence or burnup increases, <c>-component dislocation loops and short line dislocations emerge in neutron-irradiated Zircaloy and Zr-Nb alloys, meaning that the Burgers vector contains a <c>-component of the hcp unit cell at the expense of the <a>-component. At fluences higher than ≈3 x 10^{21} n·cm^{-2} (E > 1 MeV), <a>-type dislocations and loops diminish and <c>-type dislocations emerge.

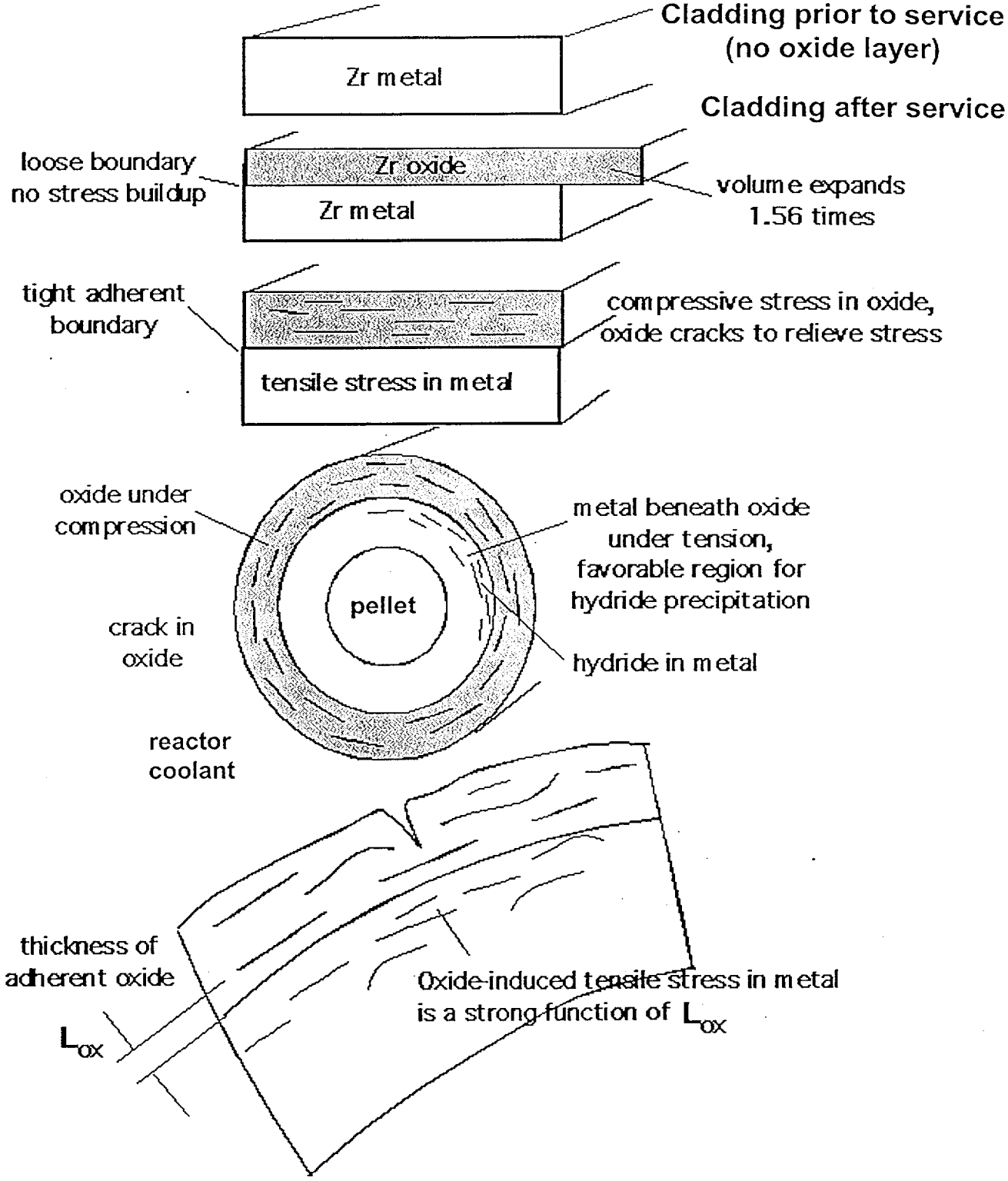

NOTE: Oxide-induced residual stress in metal is a function of thickness of uncracked adherent oxide (L_{ox}) in contact with metal.

Figure 2. Schematic Illustration of Origin of Oxidation-Induced Residual Stress in CSNF Cladding Metal and Characteristic Oxide Cracking and Hydride Concentration Beneath Cracked Oxide

The nature of this transition, interaction of impurities with irradiation damage, impurity segregation to defect clusters, and associated phase transformation have significant effects on the mechanical properties of CSNF cladding.

6.2.5 Radiation Annealing Hardening (RAH)

Irradiated Zr and Zircaloys are susceptible to RAH. The phenomenon refers to hardening of irradiated Zr and Zr-base alloys when they are annealed at a certain temperature range (≈320-370°C) in the absence of neutron flux (Snowden and Veevers 1973; Onchi et al. 1980; Onchi et al. 1983). The phenomenon has been reported for both BWR (Adamson and Bell 1985; Chung 1987) and PWR (Chung 1987; Garde 1989) SNF cladding. It has been attributed to interaction and segregation of oxygen to dislocations and defect clusters (Adamson and Bell 1985; Chung 1987) or to irradiation-induced precipitation of oxygen-rich phases (Chung 1987). Radiation anneal hardening will occur in CSNF cladding under repository conditions if the cladding temperature reaches ≈320-350°C as illustrated in Figure 1.

6.2.6 Hydrogen Uptake and Solubility Limit

In PWR cladding, ≈12-18% of all hydrogen atoms that are generated from the oxidation process is picked up from the coolant side of the cladding (Garde 1989). According to McMinn et al. (1998), the solubility limit of hydrogen in irradiated Zircaloy is ≈90-100 wppm at ≈325°C. Therefore, hydrogen up to ≈100 wppm will be dissolved in the metal as solutes at ≈325°C. On further operation (i.e., more corrosion and more hydrogen uptake), hydrides start to precipitate on the habit plane while the concentration of hydrogen in solid solution at ≈325°C remains at ≈100 wppm. However, the total concentration of hydrogen present in the hydrides, oxide layer, and solid solution in standard Zircaloy-4 PWR cladding can be anywhere from 30-800 wppm, depending on fuel burnup, coolant temperature, oxidation, and axial position in the fuel rod.

6.2.7 Hydride Precipitates

The habit plane of hydride precipitates in Zircaloy was determined by Westlake (1968) to be {107}. In α-phase Zr, the {107} plane is only 14.7° away from the basal plane, {001} or {002}. Therefore, the basal plane is a useful reference plane for the habit plane of hydride precipitation in Zircaloy cladding. As a result of the crystallographic relationships between the habit plane of hydrides and the texture of commercial fuel cladding, most hydrides precipitate in the circumferential direction; that is, the thickness direction of the hydride platelet (≈2-10 μm wide and ≈0.1-0.2 μm thick) is parallel to the radial direction of the cladding tube. Thus, the circumferential orientation is the natural direction of the hydride platelets that form in a PWR cladding. Under the high coolant pressure of a PWR that more than offsets the applied stress, hydride orientation is in effect determined by the texture of the cladding. Cladding texture in turn is determined primarily by the fabrication procedure of the cladding.

At high burnup, the metallic layer in contact with the coolant side oxide layer in PWR cladding usually contains high-density circumferential hydrides, while the hydride density in the midwall or in the metallic layer in contact with fuel pellets is low (see Fig. 2). Macroscopic hydride platelets distributed perpendicular to the direction of primary stress (i.e., radial hydrides) are particularly deleterious to the cladding's mechanical properties. However, this is not the case

under normal operating conditions in which hydrides mainly precipitate as platelets in the circumferential direction. Circumferential hydrides do not degrade the mechanical integrity of fuel cladding under tension.

The relatively large circumferential hydrides are usually revealed from polished and etched metallographic specimens. In addition to these "macroscopic" hydrides, which can be readily resolved by optical microscopy, other "microscopic" hydrides have been reported to be present in irradiated Zircaloy, which can be resolved only by transmission electron microscopy (Chung 1987). These "microscopic" hydrides, ≈20-80 nm thick and ≈100-500 nm long, are usually associated with irradiation-induced <c>-type dislocation loops and short line dislocations, and their density increases with burnup. Both types of hydride could play an important role in the degradation of mechanical properties of CSNF cladding, especially at high burnup.

Macroscopic hydrides are δ hydrides (an fcc structure). The δ hydrides form under equilibrium or near-equilibrium conditions and have a stoichiometry close to $ZrH_{1.60}$. Like the circumferential hydrides, hydrides that are oriented radially or diagonally are also δ hydrides. Microscopic hydrides resolved by transmission electron microscopy have also been reported to be δ hydrides (Chung 1987).

According to the study by Simpson and Cann (1979), fracture toughness of δ hydrides is low, ≈1 MPa $m^{0.5}$ at 23°C and 1-4 MPa $m^{0.5}$ at ≈300°C. The large scattering at ≈300°C is not well understood. A similar level of fracture toughness is also expected for a hydride blister, which is also a δ hydride.

6.2.8 Residual Stress

The metallic layer in contact with the waterside oxide layer is subject to residual stress, which is produced by the expansion of Zr oxide volume; that is, the Pilling-Bedworth ratio of Zr is as large as ≈1.56 (see Fig. 2). The oxidation-induced residual stress can be calculated to a first approximation by the method shown in Figure 3. Results of such conservative calculations, summarized in Table 2, indicate that stress intensity on a flaw in the metallic layer (in contact with the coolant-side oxide layer) is a strong function of the thickness of the adherent uncracked oxide (denoted as L_{ox} in Figs. 2 and 3) that contains a high volume fraction of tetragonal ZrO_2. The typical thickness of the adherent uncracked oxide ranges from ≈2 to ≈4 μm for PWR SNF cladding (Newman 1986; Garde et al. 1996).

During hot-cell burst tests of PWR SNF cladding in inert gas environment at 290-325°C, cracks always initiated on the outer diameter (OD) side of the cladding metal that was covered with an oxide layer (Chung and Yaggee 1984; Chung et al. 1987). No cracks were observed in the metallic region when the oxide layer was removed (Chung and Yaggee 1984). This indicates that significant oxide-induced residual stress was present in the oxide-covered metallic region. When the oxide was spalled during handling and assembling of the latter specimen, the residual tensile stress was relieved; therefore, no cracks were produced in that region. This observation lends support to the model summarized in Figure 3.

Similar to that in the oxide, a volume expansion of ≈15% occurs when Zr metal is converted to δ hydride. As a consequence, additional residual stress is generated in the metallic region

surrounding a hydride. Dislocations are frequently observed near a hydride platelet, especially in the relatively soft unirradiated Zircaloys. This is a consequence of shear stress that is developed between the metal and the hydride in the direction parallel to the hydride platelet. When circumferential hydrides are packed closely as in the OD-side metallic region in a high-burnup PWR cladding, a significant level of compressive stress is produced in the direction perpendicular to the hydride platelets (i.e., in the radial direction of the cladding wall).

Table 2. Estimated Oxide-Induced Residual Stress and Stress Intensity for Flaws in Metallic Layer in Contact with Coolant-side Oxide Layer of PWR SNF Cladding (applied stress of ≈138 MPa based on conservative fuel conditions at ≈60 MWd/kgU)

For Lox ≈3 μm			
Flaw size	1 μm	10 μm	100 μm
Residual stress (MPa), from Figure 3	200	200	200
Total stress (MPa)[a]	338	338	338
Stress intensity (MPa $m^{1/2}$), from Equation 1	0.4	1.3	4.2
For Lox ≈10 μm			
Flaw size	1 μm	10 μm	100 μm
Residual stress (MPa), from Figure 3	660	660	660
Total stress (MPa) [a]	798	798	798
Stress intensity (MPa $m^{1/2}$), from Equation 1	1.0	3.2	10.0

[a] Total stress = residual stress + applied stress

6.2.9 Stress State

Another important characteristic of CSNF cladding is the multiaxial state of stress in the metallic region in contact with the coolant-side oxide layer. Schematically illustrated in Figure 4, the stress is related to the residual stress produced by the large expansion in volume of ZrO_2 (Pilling-Bedworth ratio ≈1.56) and δ hydride (Pilling-Bedworth ratio ≈1.15). The oxidation-induced volume expansion produces stress components in axial and tangential directions in the metallic region in contact with the oxide layer. The residual stress in the tangential direction is then superimposed on the stress produced from rod internal pressure. In addition to this, because of high volume fraction of circumferential hydrides, significant level of compressive stress can be produced at high burnup in the radial direction in the metallic region beneath the oxide layer.

Because the stress is multiaxial, a crack or a flaw in the OD-side metallic region will be subject to mixed-mode loading (i.e., either Modes I and II or Modes I and III) rather than a simple Mode-I loading (see Fig. 5). Most laboratory-simulated tests of DHC were conducted under Mode-I loading conditions, in which crack propagation is more difficult than under mixed-mode loading conditions under otherwise similar situation.

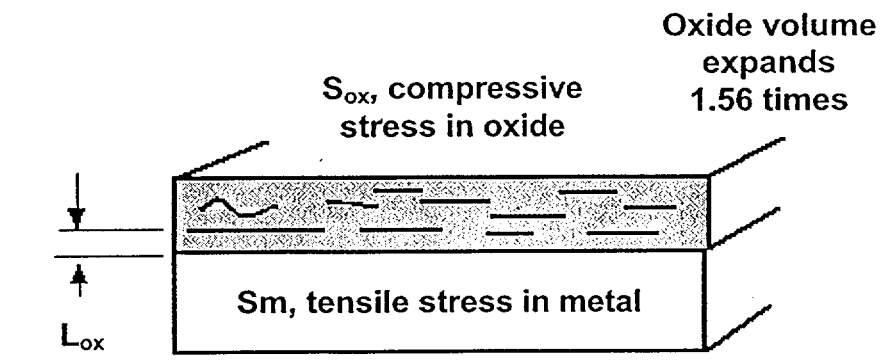

m	metal
ox	oxide
E	Young's modulus
X	elastic strain
Hm	metal layer thickness
L_{ox}	adherent oxide thickness
S	oxidation-induced stress
W	common width of layer

$Sm\ Hm\ W + S_{ox}L_{ox}\ W = O$
$Sm = Em\ Xm$ (tensile stress in metal
$Em\ Xm\ Hm = E_{ox}\ (0.56/3 - X_{ox})\ L_{ox} = O$
X_{ox} = negligible
E_{ox} = 200 GPa
Hm = 560 μm for PWR high-burnup cladding

Sm (in MPa) = 66 L_{ox} (L_{ox} in μm)

Figure 3. Summary of Model Designed to Calculate Residual Stress in CSNF Cladding Metal as a Result of Oxide Volume Expansion and Circumferential Cracking of Oxide

6.2.10 Annealing-Out of Residual Stress under Repository Conditions

The residual stress associated with OD-side oxide layer and hydrides in the outer metallic layer (in contact with the oxide layer) may or may not be significantly annealed out during the heatup phase under repository conditions (e.g., during the first 100 years or so after closure).

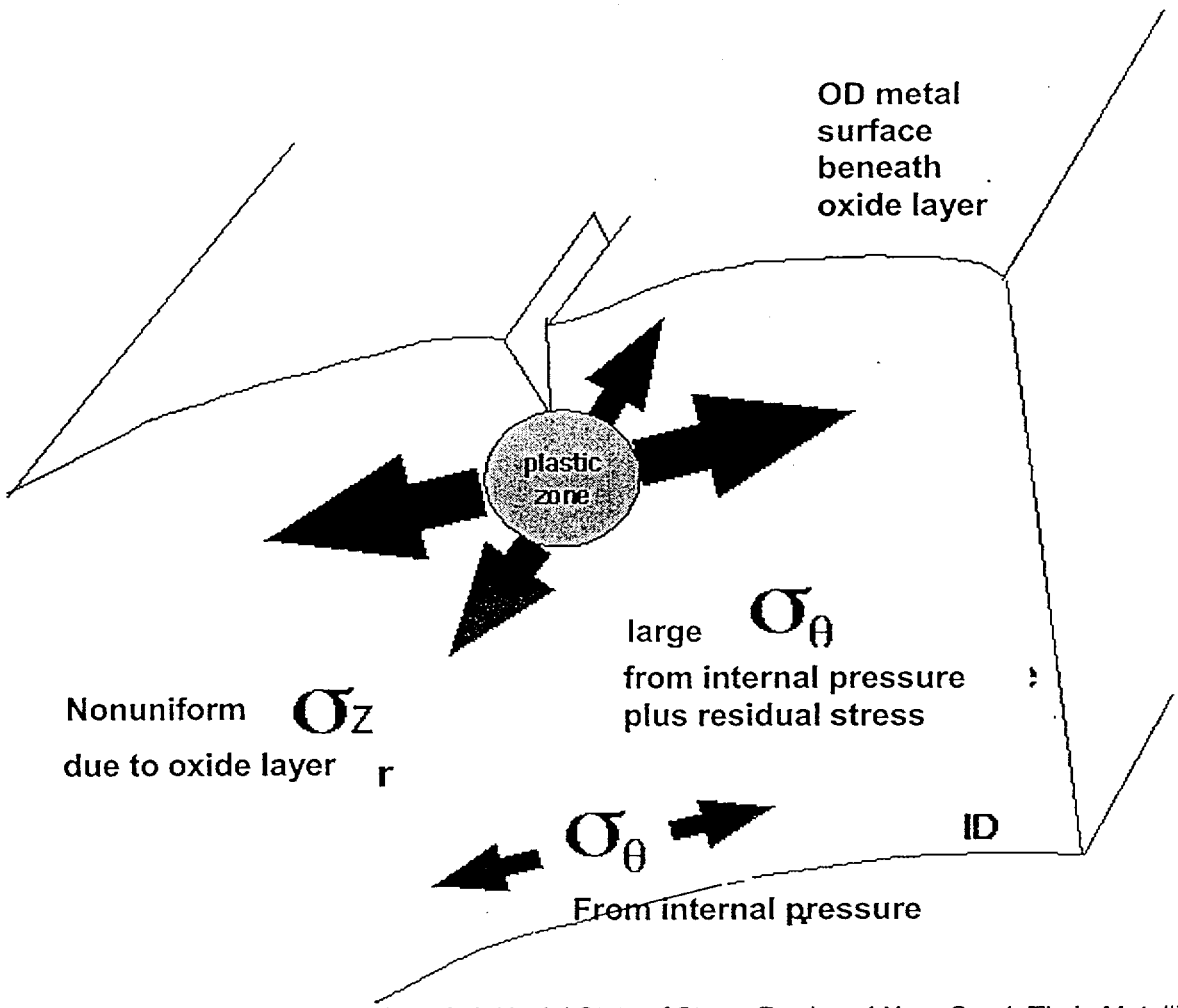

Figure 4. Schematic Representation of Multiaxial State of Stress Produced Near Crack Tip in Metallic Region of CSNF Cladding in Contact with Waterside OD-side Oxide Layer

More than any other factors, the peak cladding temperature is the single-most important factor that influences this process. Slow diffusion of oxygen solutes from the OD to the inner diameter (ID) side of the cladding occurs at the same time; therefore, the thickness of the brittle oxygen-rich outermost metallic layer will also increase.

6.2.11 Recovery of Irradiation Hardening under Repository Conditions

In an investigation of the behavior of dry-stored PWR SNF cladding, Einziger and Kohli (1984) summarized results of microhardness measurements that were intended to determine the degree of recovery of irradiation-induced hardening. The results show a significant recovery at 300-350°C for specimens irradiated at 40-60°C and a more pronounced recovery at 417°C for specimens irradiated at 216-267°C. This is consistent with the generally accepted trend that significant recovery of irradiation-induced hardening occurs at temperatures higher than the irradiation temperature.

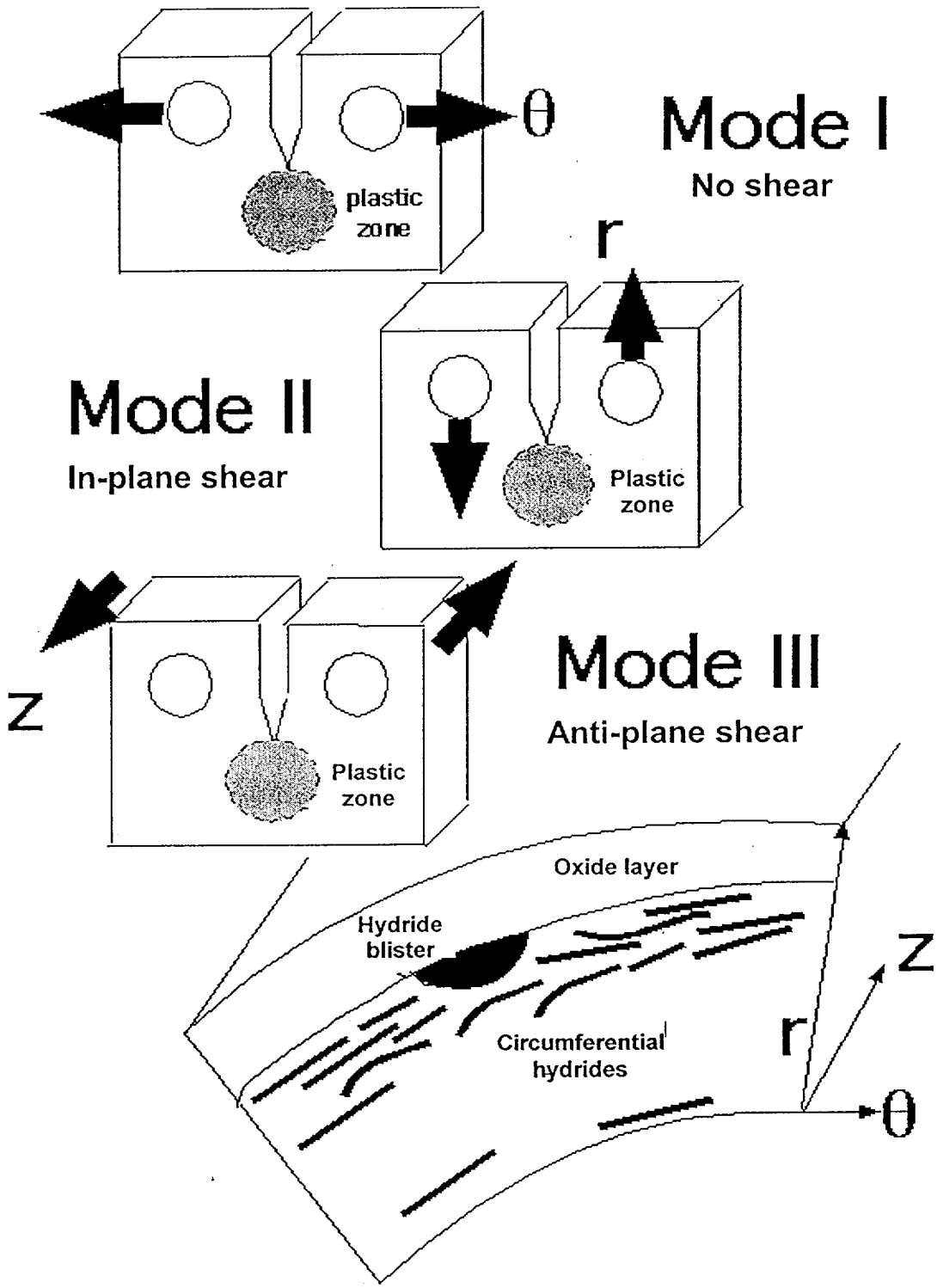

Figure 5. Schematic Illustration of Mode I, II, and III Loading on Compact Tension Specimens

In contrast, no or negligible recovery was observed for PWR SNF cladding after annealing at 320-323°C (same as the irradiation temperature) for up to ≈2,000 h. Considering these

observations, it is difficult to conclude that significant or full recovery of irradiation-induced hardening will occur under repository conditions.

Understanding the potential annihilation of irradiation-induced damages, radiation-anneal hardening, the potential recovery of irradiation-induced hardening, and annealing-out of residual stress has significant implications in understanding many aspects of the long-term performance of CSNF cladding under repository conditions, e.g., DHC, hydride reorientation and juvenile stress-rupture, creep, and mechanical failure from rock fall.

6.3 DELAYED HYDRIDE CRACKING

6.3.1 Introduction

DHC is a proven field event for Zircaloy-2 and Zr-2.5%Nb pressure tubes in CANDU reactors (Chow and Simpson 1986; Cheadle et al. 1987). Cracking of Zircaloy-2 (Chow and Simpson 1986; Coleman et al. 1989) and Zr-2.5Nb pressure tubes (Chow and Simpson 1986; Cheadle et al. 1987; Moan et al. 1990) and DHC-related metallurgical processes have been investigated extensively in the past, namely, hydriding behavior (Simpson and Cann 1979; Coleman 1982; Yuan and Tangri 1982; Davies and Stearns 1986; Leger et al. 1989), hydride blister (Chow and Simpson 1986; Leger et al. 1989), irradiation-induced impurity segregation (Aitchison and Davis 1993), fracture toughness (Chow and Simpson 1986; Wallace et al. 1989; Chow et al. 1991), subcritical crack growth (Simpson and Puls 1979; Puls et al. 1982; Shi and Puls 1996), and ductile-brittle-transition (DBT) phenomenon (Davies and Stearns 1986; Chow and Simpson 1986; Coleman et al. 1989).

Laboratory simulation tests of DHC in unirradiated hydrided Zircaloy fuel cladding have been reported only recently by several investigators (Efsing and Petterson 1996; Grigoriev and Josefsson 1998). The objectives of these studies on precracked cladding specimens were to provide a better understanding of the phenomenon of long axial splitting that has been observed in defective Zircaloy-2 fuel cladding in some BWRs.

Since the majority of these investigations were conducted under laboratory conditions, it is important, however, to recognize that a large portion of the data on DHC initiation and crack propagation was obtained on unirradiated hydrogen-charged specimens under relatively simple loading and thermal conditions. Most of the accelerated laboratory tests were conducted primarily to obtain data on crack growth rates which are crucial to the evaluation of leak-before-break behavior during a pressure tube failure in a CANDU reactor.

Based on investigations on unirradiated-hydrided Mode I compact-tension specimens, DHC has been established as the mechanism of slow subcritical crack growth in unirradiated pressure tubes. However, quantitative understanding of the initiation phase of DHC is relatively poor, even though the initiation process is more important than crack propagation for evaluation of the potential susceptibility of CSNF cladding to DHC under repository conditions.

6.3.2 Accelerated DHC Experiments in Laboratory

The cracking behavior of a hydrogen-charged precracked compact-tension specimen, tested under accelerated laboratory conditions, can be considered to occur in three stages, as shown

schematically in Figure 6. When stress intensity is lower than a threshold level, commonly referred to as K_{IH}, an incipient crack or flaw is stable and does not grow. When stress intensity exceeds the critical level K_{IH} but is lower than the fracture toughness K_{IC}, a crack grows slowly at a stable rate. When stress intensity is greater than the fracture toughness K_{IC}, an unrestrained fast crack propagation occurs. Critical stress intensity is determined by:

$$K_{IH} = \sigma(a\pi/2)^{0.5} \quad (1)$$

where, K_{IH} critical (or threshold) stress intensity for DHC propagation (in MPa $m^{0.5}$)
σ stress (in MPa)
a crack size (in m).

The stable subcritical crack growth for the stress-intensity range $K_{IH} < K < K_{IC}$ is attributed to DHC, a process that repeats a cycle in which hydrogen solutes diffuse to the crack tip, hydrides precipitate at or near the crack tip, and, subsequently, the hydrides or the metallic region near the hydrides crack under stress and, thus, leads to a slowly advancing macroscopic crack. This process must satisfy the following conditions: stress intensity must exceed the threshold level K_{IH}, local hydrogen buildup must be sufficiently large to exceed the terminal solubility at the crack tip and induce hydride precipitation, and a sufficient level of hydrogen solutes must be present in the metal near the advancing crack to allow migration of hydrogen to the stress-intense crack tip. Coleman (1982) showed an elegant example of hydrides that had precipitated in front of the advancing crack tips in compact tension specimens.

In the laboratory testing of crack propagation via DHC mechanism, crack growth rate and threshold stress intensity K_{IH} were measured at constant temperature. Furthermore, test conditions of most of these simplified accelerated studies of DHC are characterized by several other aspects, i.e., unirradiated hydrided specimens, Mode I compact-tension specimens, little or no residual stress in the specimens, negligible driving force for hydrogen diffusion due to temperature gradient, and short test duration (i.e., typically less than several days versus 10-20 years for DHC in CANDU pressure tubes, and long-term for SNF cladding in a waste repository). Based on laboratory studies of this type, a threshold stress intensity K_{IH} of 5.5-8.0 MPa $m^{0.5}$ was reported for CANDU pressure tube materials (Simpson and Puls 1979; Puls et al. 1982; Davies and Stearns 1986; Shi and Puls 1996).

In contrast, Efsing and Petterson (1996) reported somewhat higher value of K_{IH} of 7.5-9.0 MPa $m^{0.5}$ for unirradiated hydrided Zircaloy-2 at ≈300°C that had 500-1,000 wppm hydrogen and yield strength of 500-650 MPa. It is not clear whether the seemingly greater K_{IH} for the relatively thin fuel cladding specimens is attributed to specimen thickness, test method, texture, or a combined effect of these factors. It is likely that the greater value of K_{IH} is very much associated with the very thin wall thickness of the test specimens.

The applied stress (due to internal gas pressurization) in CANDU pressure tubes and the maximum projected applied stress in PWR cladding metal (for a fuel burnup ≈60 MWd/kgU) is comparable, i.e., ≈140 and ≈135 MPa, respectively.

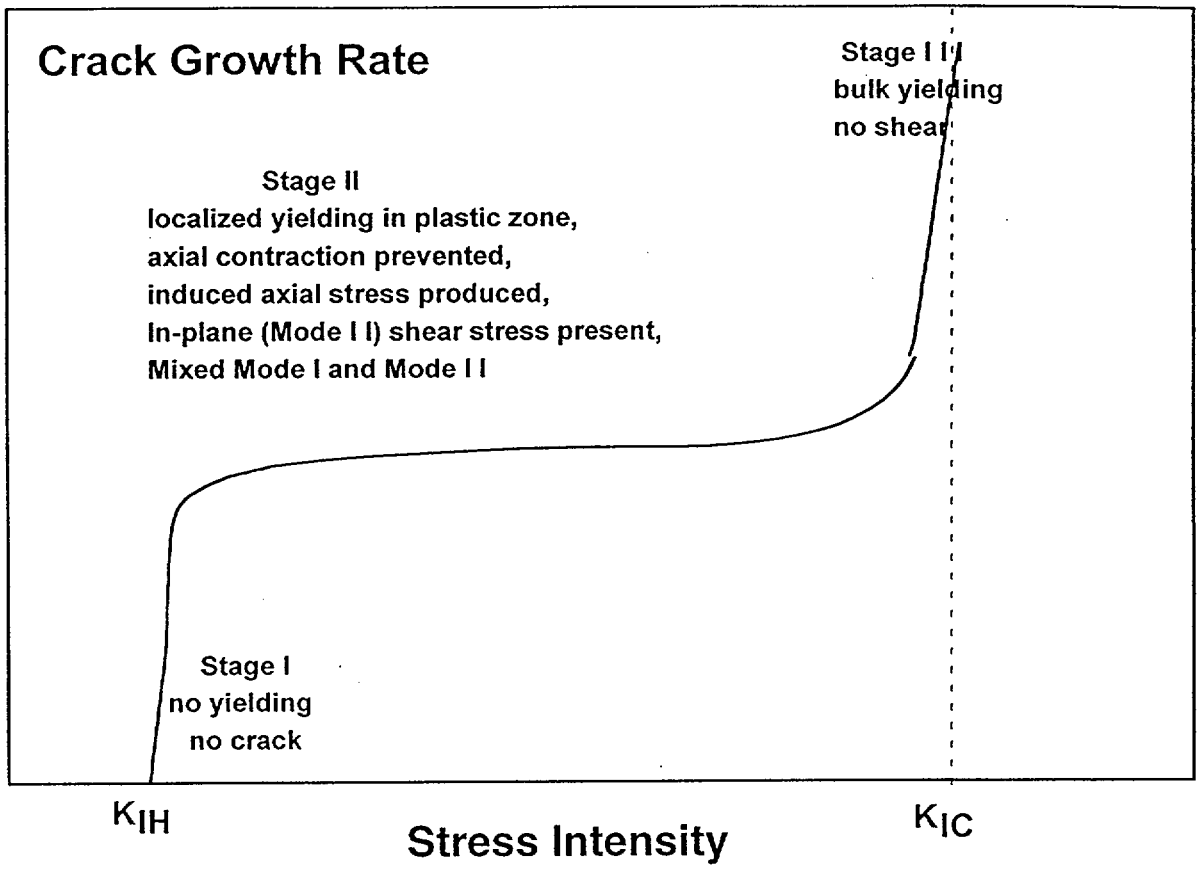

Figure 6. Crack Growth Rate versus Stress Intensity Typical of Accelerated Laboratory Testing of DHC of Compact-Tension Specimens

To facilitate a more direct comparison, the metallurgical factors that are relevant to DHC for the only known field event (i.e., CANDU pressure tube failure), simulated crack growth tests in laboratory, and PWR SNF cladding under repository conditions are summarized in Table 3.

6.3.3 Prediction of DHC in CANDU Pressure Tube Based on Laboratory-Measured K_{IH}

The size distribution of flaws on the outer surface of a CANDU pressure tube is not known. However, the OD surface of a pressure tube is covered with a thin oxide layer that is in tight contact with the underlying metal, and as a result, the metal/oxide boundary is relatively smooth and is free of large flaws. In consideration of this, the flaw size on the OD metal is conservatively estimated to be no larger than ≈50 μm. Based on this flaw size and an applied stress of ≈140 MPa, a simple calculation (Eq. 1) shows that maximum stress intensity in a CANDU pressure tube (OD surface) is no greater than ≈1.7 MPa $m^{0.5}$, far smaller than the threshold stress intensity K_{IH} of ≈5.5 MPa $m^{0.5}$ determined from accelerated laboratory experiments.

Therefore, the occurrence of DHC in a CANDU pressure tube (a horizontal component), cannot be predicted from a simple model based on the results of accelerated laboratory tests. This

conclusion is not surprising if one realizes that the accelerated isothermal tests in the laboratory were primarily intended to measure DHC crack growth rate rather than to understand crack initiation under CANDU operating conditions.

The above simple analysis suggests that great caution must be exercised in applying a similar model to predict or refute the occurrence of DHC in CSNF cladding under repository conditions. Crack initiation in failed CANDU pressure tubes occurred, in fact, not in association with fabrication-related flaws but in association with hydride blisters that formed during operation on the OD side of the tube (Chow and Simpson 1986; Cheadle et al. 1987; Leger et al. 1989; Coleman et al. 1989; Moan et al. 1990). That is, microstructural evolution which occurred on the OD side surface over a period of ≈10-20 years was the key in crack nucleation in the failure CANDU pressure tubes.

6.3.4 Comparisons of DHC-Relevant Parameters in CANDU Pressure Tube, Laboratory Compact-Tension Specimen, and CSNF Cladding

The difference in crack initiation behavior in CANDU pressure tubes and compact-tension laboratory specimens highlights the importance of the long-term microstructural evolution associated with DHC initiation. The key aspects of DHC initiation in CANDU pressure tubes can be divided into several processes, i.e., sagging of the hot pressure tube (maintained in a horizontal position at ≈300°C), contact of the pressure tube OD with the horizontal cold calandria tube (temperature ≈70°C), hydrogen migration to the cold contact spot, nucleation of a hydride blister, growth of the hydride blister, crack initiation in the blister, crack growth in the blister, and adjacent metal. Qualitatively, these processes are understood fairly well (Chow and Simpson 1986; Coleman et al. 1989; Cheadle et al. 1987; Moan et al. 1990; Shi and Puls 1996).

In the crack nucleation process, note that K_{IH} in the field conditions could be in fact close to the K_{IH} of the delta hydride blister, i.e., 1-3 MPa $m^{0.5}$ (Simpson and Cann 1979) because a majority of cracks in failed CANDU pressure tubes are known to have nucleated at large hydride blisters produced on the OD surface.

Quantitative aspects of DHC initiation in CANDU pressure tubes as reviewed by Shi and Puls (1996) are, however, still not well understood. A quantitative understanding of DHC initiation, rather than crack propagation, would certainly be the key feature that is required for predicting or ruling out DHC in relatively thin SNF cladding under repository conditions. The relative importance of the initiation phase of DHC cannot be overemphasized, especially when we consider long-term nature of potential microstructural evolution under repository conditions.

Table 3. Factors that Influence DHC in CANDU Pressure Tubes, Compact-Tension Laboratory Specimens, and High-Burnup PWR Cladding in Repository

Factor	CANDU Reactor Pressure Tube	Compact Tension Specimen	PWR SNF Cladding in Repository
Material	Zr-2.5Nb or Zircaloy-2	Zr-2.5Nb, Zircaloys	Zircaloy-4
DHC Proven	yes	yes	no
Time to Occur	many years	< several days	not known
Hydrogen Source	coolant and moisture, virtually unlimited	precharged hydrogen	H dissolved in cladding, limited
DHC Initiation Spot	OD hydride blisters	precrack tip	not known
Temperature Difference near Cold Spots	large (≈200°C) at calandria contact spots	negligible	small, not known
Stress Gradient	low	high	not known
Primary Driving Force for Hydrogen Migration	Temperature gradient	Stress gradient	stress gradient plus temperature gradient
Hydride Blistering	yes	no	not known
Hydrides Concentrated in Local Spots	yes, precursor to blistering	radial hydrides near crack tip	limited to some spots in highly oxidized standard Zircaloy-4 at high burnup
Locally Concentrated Oxygen in Metal	OD region beneath oxide layer	absent or negligible	OD region in contact with oxide
Applied Stress (MPa)	≈140	high	≈60-135 MPa
Residual Stress	some	negligible	multiaxial residual stress

6.3.5 Potential for DHC Initiation at Inner Diameter of CSNF Cladding

Most incipient cracks in SNF cladding, produced mostly as a result of pellet-cladding interaction or pellet-cladding mechanical interaction, are on the ID side, i.e., on the pellet side. The potential for collecting hydrogen, concentrated hydride precipitation, and hydride blistering in the ID region is insignificant or negligible, because the temperature is higher than the OD region and, hence, the thermal driving force for hydrogen collection is either absent or negligible. Therefore, the conditions are similar to those of the isothermal simulation tests conducted in laboratory (Simpson and Puls 1979; Puls et al. 1982; Davies and Stearns 1986; Shi and Puls 1996), and the conservative value of critical stress intensity of ≈5.5 MPa $m^{0.5}$ (Table 1) can be used to predict potential propagation of the incipient cracks.

Oxide- or hydride-associated residual stress on the ID side is also small; therefore, the maximum applied stress on this side will not exceed ≈135 MPa, even for a burnup as high as ≈60 MWd/kgU. Therefore, from Equation 1, it is calculated that for an incipient crack on the ID side to propagate via the DHC mechanism, the crack size must exceed ≈1,000 μm which is greater than the thickness of a PWR fuel cladding wall itself (i.e., 570-635 μm). Therefore, initiation and propagation of DHC on the ID side is not a concern under repository conditions.

6.3.6 Potential for DHC Initiation at Outer Diameter of CSNF Cladding

Because of the variations in the geometry of cladding and pellet, cladding oxide layer thickness, hydride distribution, heat generation from pellet, heat transport, and cooling, some regions of CSNF cladding under repository conditions will be cooler than other regions. Although expected to be small, the temperature nonuniformity will be significantly more pronounced at the OD than at the ID side of the cladding. Therefore, there could be some degree of driving force for hydrogen solutes to migrate over a long period of time from the hotter regions to the cooler regions of cladding metal, under either temperature or stress gradients or both.

The key process for potential DHC initiation at the OD side is then potential long-term microstructural evolution, i.e., nucleation, growth, and cracking of hydride blisters in the metallic region, especially on some types of localized hydrogen-collecting spots. That is, susceptibility to DHC will be determined essentially by the hydride-related microstructural evolutions that may occur over a long term in a repository. The hydrogen-collecting spots, characteristically cooler (see e.g., Newman 1986) and higher in stress, or both, could be locations near pellet-pellet boundaries, near pellet-pellet gaps (i.e., the gap produced as a result of fuel densification), beneath a spacer grid, or beneath a spalled oxide layer. These potential DHC initiation spots are illustrated schematically in Figure 7.

Microstructural evidence of the presence of concentrated hydrides near pellet-pellet boundaries and gaps has been reported for some high-burnup PWR claddings that were stored and examined in hot cells. Evidence of concentrated hydrides at pellet-pellet interfaces has been reported by Smith et al. (1994) and Garde et al. (1996). Evidence of concentrated hydrides at pellet-pellet gaps was reported by Yang et al. (1991) and Garde et al. (1996). Evidence of formation of hydride blisters beneath a spalled oxide layer was reported by Guedeney et al. (1991), Garde et al. (1996), Lemoine et al. (1997), Papin et al. (1996), and Meyer et al. (1996).

However, all of this evidence of concentrated hydrides was observed only in PWR SNF cladding fabricated from standard Zircaloy-4 (composition in wt.%: 1.5 Sn, 0.2 Fe, 0.01 Ni, and 0.1 Cr) and operated to burnups higher than ≈55 MWd/kgU. Oxidation and hydriding in standard Zircaloy-4 cladding are well known to be high at high burnup (≥ 55 MWd/kgU). In contrast, the degree of oxidation and hydriding in more advanced fuel claddings commonly used these days in LWRs, such as low-Sn (Sn content ≈1.3 wt.%) Zircaloy-4, optimized Zircaloy-4, Zirlo (a Zr-1Sn-1Nb-0.1Fe alloy), M5 (a Zr-1Nb alloy), and optimized Zircaloy-2, is relatively low even at high burnup. Therefore, for the purpose of present analysis, hydride-related degradation of CSNF cladding fabricated from standard Zircaloy-4 can be considered as a conservative bounding case.

Even for PWR cladding fabricated from standard Zircaloy-4 no evidence for concentrated hydrides has been reported for low (<25 MWd/kgU) or medium (25-55 MWd/kgU) burnup. Therefore, formation of locally concentrated hydrides is limited to a small fraction of PWR cladding fabricated from standard Zircaloy-4 and operated to burnups higher than ≈55 MWd/kg. Consequently, although we cannot rule out or predict clearly at this time that a hydride blister forms and grows near such locally concentrated hydrides under repository conditions, the potential for initiation of DHC near such concentrated hydrides is at any rate predicted to be insignificant for the majority of commercial spent fuels.

6.3.7 Influence of Oxide Cracking under Long-Term Creep

One type of cladding region that could potentially "collect" hydrogen solutes and lead to locally concentrated precipitation of hydrides consists of radially penetrating cracks in the oxide that extend to the metallic layer. Radial oxide cracks may or may not be produced as a result of long-term creep deformation of the cladding under repository conditions. This situation is shown schematically in Figure 8. Occurrence of radial cracks in the oxide layer was reported by Einziger and Kohli (1984) for PWR SNF cladding (burnup ≈27-31 MWd/kgU) under dry storage conditions, although their cladding was pressurized to an unrealistically high level of applied stress of ≈143 MPa at ≈323°C for up to ≈87 days.

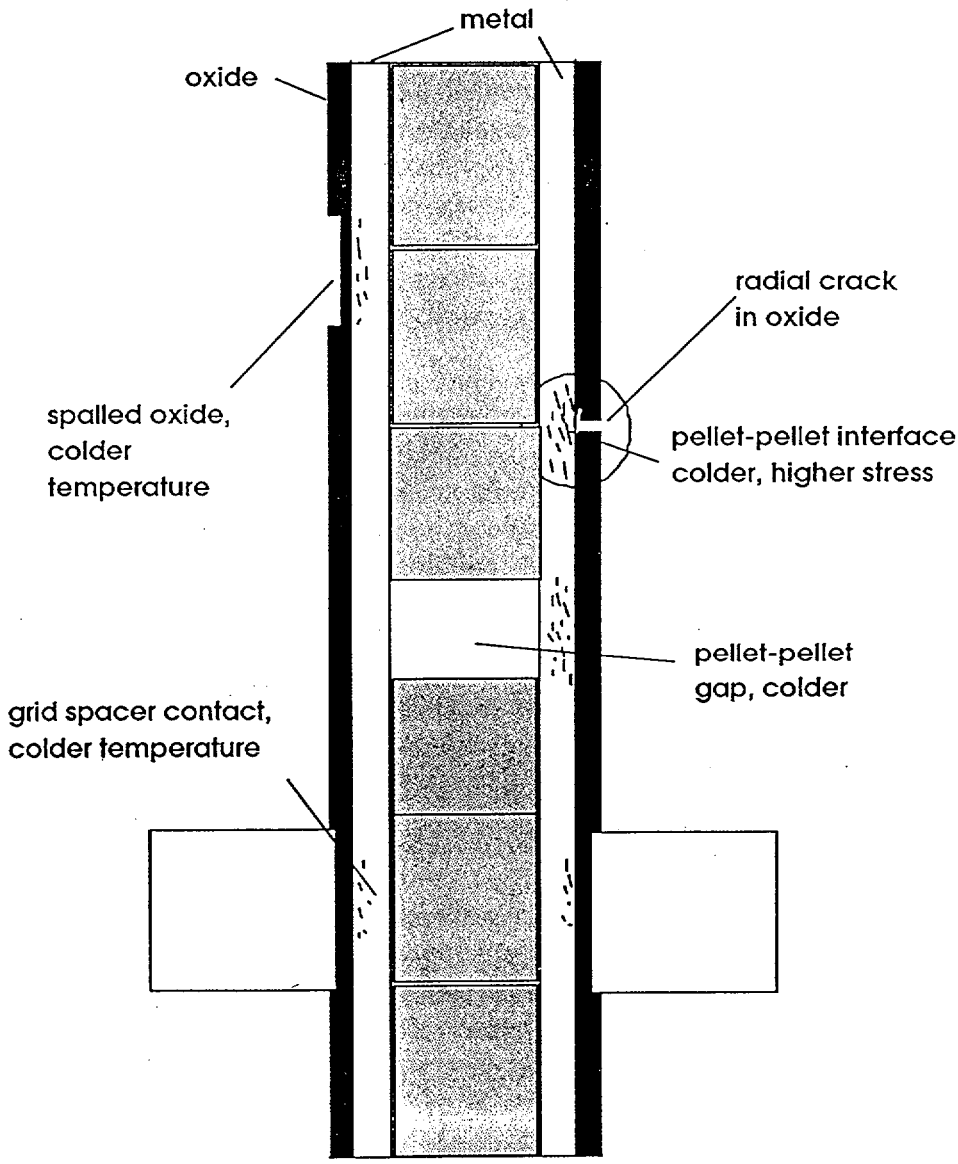

Figure 7. Schematic Illustration of Potential Spots for Concentrated Precipitation of Hydrides that may Lead to Hydride Blistering in High-Burnup PWR Cladding in Waste Repository

An important factor related to potential creep-induced oxide cracking is the long-term evolution of microstructure and strength of the cladding metal (discussed in Sections 6.2.10 and 6.2.11). The potential for formation and growth of a hydride blister and the subsequent initiation of DHC near such an oxide crack are difficult to predict at this time, because the degree of creep deformation in the oxide, the magnitudes of temperature and stress gradients in the metal beneath such a radial crack, and potential localized corrosion in such a metallic region are not known.

Significant level of residual stress is produced during welding of the end caps. However, the temperature of the end plug weld is relatively low, and as a result, the oxide layer accumulated on the end plugs is very thin. Therefore, radial oxide cracking in end cap welds is not likely to occur.

6.4 HYDRIDE REORIENTATION

The behavior of CSNF cladding under dry storage conditions has been studied by several investigators (Einziger and Kohli 1984; Peehs and Fleisch 1986). In one study, Einziger and Kohli (1984) reported observation of significant hydride reorientation in PWR cladding (burnup ≈27-31 MWd/kgU) after testing at ≈323°C in a hot cell, i.e., a transition of the hydride structure from predominantly circumferential orientation to radial orientation. This observation is consistent with results of studies on unirradiated hydrided specimens of Zr and Zr-base alloys under laboratory conditions (Marshall 1967; Bai et al. 1994; Chan 1996).

The phenomenon of hydride reorientation consists of dissolution of the normal circumferential hydrides as the temperature is increased higher than the heatup solubility limit, and precipitation of radial hydrides as the temperature is decreased below the cooldown solubility limit under stress. Nonequilibrium thermodynamic processes and deformation during hydride precipitation have been modeled by Stout (1989). According to McMinn et al. (1998), the heatup and cooldown solubility limits differ significantly, the mechanism of which is not well understood.

The reorientation of hydrides is strongly influenced by the stress (Marshall 1967; Bai et al. 1994; Chan 1996; Hardie and Shanahan 1975) and texture (Coleman 1982) of the cladding. However, the effect of cooling rate has been reported to be insignificant (Chan 1996). Therefore, the minimum stress for reorientation that is applicable to spent irradiated cladding is of particular importance.

6.4.1 Minimum Stress for Hydride Reorientation

The minimum stress for hydride orientation in unirradiated hydrided specimens has been reported to be ≈85-95 MPa (Marshall 1967; Bai et al. 1994; Chan 1996). In contrast, Hardie and Shanahan (1975) reported unusually low threshold stress of only ≈35 MPa for Zr-2.5Nb pressure tube specimens. However, the texture of their test specimen was entirely different from that of CSNF cladding, that is, the basal pole in the former material was ≈90° away from the radial direction (i.e., basal plane nearly parallel to radial direction of the tubing), whereas the basal pole of the latter is ≈30° away from the radial direction (i.e., basal plane nearly perpendicular to radial direction). Because the basal plane is nearly parallel to the habit plane of hydride precipitation (Section 6.2.7), radial hydrides in the former material are inherently easier to precipitate than in

the latter material. Therefore, the minimum stress of ≈35 MPa reported in the study of Hardie and Shanahan is not applicable to CSNF cladding.

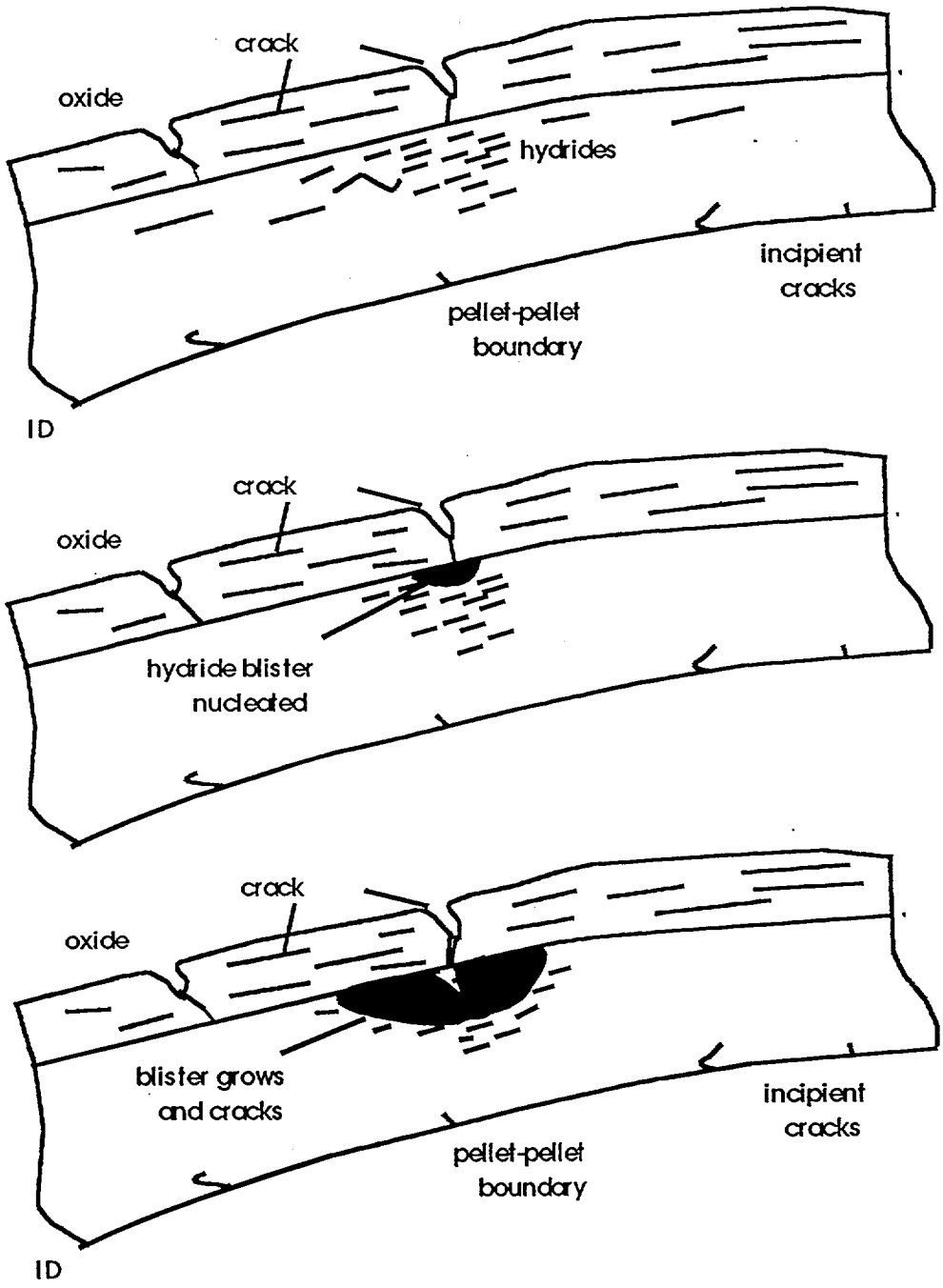

Figure 8. Illustration of Potential Oxide Cracking and Initiation of DHC in High-Burnup PWR Cladding

Einziger and Kohli (1984) observed reoriented (radial) hydrides in PWR cladding that was heated at ≈323°C for up to ≈2100 h (≈87 days) and then cooled at a rate of ≈5°C/h under an applied internal stress of ≈143 MPa. Fuel burnup was ≈27-31 MWd/kgU. This level of stress

exceeds significantly the minimum stress of ≈85-95 MPa that was observed for unirradiated hydrided specimens (Marshall 1967; Bai et al. 1994; Chan 1996).

Partial orientation of dense OD circumferential hydrides was also reported by Papin et al. (1996) for a PWR fuel (burnup ≈64 MWd/kgU) under a very fast power ramping condition that simulated a reactivity-initiated accident. Maximum cladding temperature reached in the experiment was estimated to be ≈344°C, although peak stress was not known. However, the cladding remained intact despite a measured circumferential strain of ≈1.1%.

In view of this information, reorientation of hydrides is expected to occur in medium- and high-burnup PWR cladding under repository conditions.

6.4.2 Failure Stress of Hydride-Reoriented CSNF Cladding

From the standpoint of structural integrity, the threshold stress for failure of hydride-reoriented CSNF cladding is more important than the phenomenon of hydride reorientation itself. A data base for such stress, however, is not available in the literature except for the experiment of Einziger and Kohli (1984). In that experiment, in spite of the fact that extensive reorientation of hydrides occurred when the PWR cladding (fuel burnup ≈30 MWd/kgU) specimen was exposed to ≈323°C for ≈87 days and then cooled down at a rate of ≈5°C/h, the specimen remained intact under an applied stress of ≈143 MPa. The temperature of ≈323°C is similar to the maximum design cladding temperature that is expected for CSNF cladding under repository conditions. Therefore, the experiment of Einziger and Kohli can be viewed as a bounding case (a conservative upper bound) from the standpoint of the degrading effect of hydride reorientation on cladding structural integrity.

Literature data on failure stress of as-irradiated PWR SNF cladding is summarized in Table 4. For test temperatures in the range of 315-325°C, burst strength of standard-Zircaloy-4 PWR SNF cladding increases significantly with increasing fuel burnup, i.e., from ≈400 MPa at ≈28 MWd/kgU (Chung et al. 1987) to ≈850 MPa at ≈60 MWd/kgU (Garde 1989, Garde et al. 1996, Smith et al. 1994). The as-irradiated cladding specimens tested in these internal-pressurization experiments contained few or insignificant radial hydrides before test, although a limited number of high-burnup specimens may have contained localized radial hydrides (e.g., near pellet-pellet boundaries) or even some hydride blisters beneath spalled oxide. Interestingly, Garde et al. (1996) reported that, during burst tests of ≈63 MWd/kgU PWR cladding at ≈315°C, an unusually low burst strength of ≈480 MPa was observed for one specimen that contained spalled oxide layer. Frequently, a hydride blister is produced when a fuel rod that contains spalled oxide is operated continuously to high burnup, therefore, the unusually low burst strength was most likely due to the presence hydride blister(s) in the oxide-spalled specimen.

Based on the information in Table 4, stress-rupture failure strength of the ≈30 MWd/kgU PWR cladding of Einziger and Kohli (1984) is estimated to be ≈400 MPa at ≈323°C, if hydride reorientation did not occur in the cladding. Therefore, the failure stress of the hydride-reoriented cladding would have been somewhere between ≈143 MPa and ≈400 MPa. Even the lower limit of ≈143 MPa is still significantly greater than the internal-pressure-induced stress of ≈60-80 MPa estimated for the burnup of ≈30 MWd/kg or than the internal stress of ≈90-130 MPa estimated

for the burnup of ≈60 MWd/kg. Therefore, it is concluded that even if hydride reorientation occurs in some medium- and high-burnup SNF cladding under repository conditions, subsequent stress-rupture failure in the hydride-reoriented cladding is not likely to occur.

Table 4. Failure Stress and Strain of As-Irradiated PWR Cladding (fabricated from standard Zircaloy-4, little or insignificant amount of radial hydrides) at 292-325°C, Burnup ≈22-63 MWd/kgU

Reactor and Cladding Type	Fuel Burnup (MWd/kgU)	Isothermal Test Temperature (°C)	Failure Hoop Stress (MPa)	Failure Hoop Strain (%)	Reference
Big Rock Point Zircaloy-2	22.4	325	337-514	0.4-1.1	Chung et al. (1987)
H. B. Robinson Zircaloy-4	27.7	292	498-552	2.5-11.7	Chung et al. (1987)
H. B. Robinson Zircaloy-4	27.7	325	315-469	≈2.4	Chung et al. (1987)
Fort Calhoun Zircaloy-4	41.6-53.2	315	796-823	4.5-6.9	Garde (1989)
Fort Calhoun Zircaloy-4	56.1-62.5	315	704-843	1.50-4.05	Garde (1989)
Calvert Cliffs-1 Zircaloy-4	≈63.5	315	480-983	0.58-6.47	Garde et al. (1996)
ANO-2 Zircaloy-4	55-62	315	958-1010	1.47-2.58	Smith et al. (1994) Garde et al. (1996)

7. CONCLUSIONS

1. Considering the relatively inert environment of the container and the relatively low temperature (i.e., maximum cladding temperature < 350°C) of commercial spent nuclear fuel cladding that are projected in repository, the total amount of hydrogen atoms which permeate through the oxide layer that covers the cladding surface will be insignificant. Therefore, the potential for excessive hydrogen uptake, virtual conversion of the cladding wall to hydride, and gross hydriding embrittlement is negligible or extremely small.

2. Most incipient cracks in commercial spent nuclear fuel cladding are on the ID side. Because the temperature on the ID side is higher than that on the OD side or in midwall and, hence, the thermal driving force for hydrogen concentration on the ID side is absent or negligible, the potential for collecting hydrogen solutes, concentration of hydride precipitates, and hydride blistering in the ID region is insignificant or negligible. Therefore, the condition is similar to that of isothermal laboratory simulation tests of delayed hydride cracking, and a conservative critical stress intensity of ≈5.5 MPa $m^{0.5}$ be used to predict potential propagation of incipient cracks at the ID. Based on this value of critical stress intensity and maximum stress, occurrence of delayed hydride cracking from the ID side is concluded to be unlikely. The critical stress intensity of ≈5.5 MPa $m^{0.5}$ used to reach this conclusion, is based on a set of consistent and well-accepted literature data that ranges between ≈5.5 and ≈8.0 MPa $m^{0.5}$; as such, it is a conservative value.

3. Some regions of the OD-side metal of the cladding under repository conditions will be cooler than other regions; therefore, there will be driving force for hydrogen solutes to migrate from the hotter to the cooler metallic regions at the OD side, under either temperature or stress gradients or both. The key process for potential initiation of delayed hydride cracking at the OD side, then, is long-term microstructural evolution, i.e., nucleation, growth, and cracking of hydride blisters in such metallic regions. In a certain type of PWR spent fuel cladding operated to burnups higher than ≈55 MWd/kgU, some types of localized regions at the OD side contain highly concentrated hydrides, i.e., regions near pellet-pellet boundaries, near pellet-pellet gaps, and beneath a spalled oxide layer. For such regions of concentrated hydrides in high-burnup cladding, potential for the occurrence of the chain of metallurgical processes (i.e., nucleation, growth, and cracking of hydride blisters) can be neither quantified nor ruled out at this time. In spite of this uncertainty, it is concluded that occurrence of such localized regions of concentrated hydrides is limited to a small fraction of commercial spent fuel cladding fabricated from standard Zircaloy-4 and operated in high-temperature high-duty modern PWRs to burnups higher than ≈55 MWd/kgU. Consequently, potential for initiation and propagation of a crack near such OD region of locally concentrated hydrides by delayed hydride cracking mechanism is insignificant for the majority of commercial spent nuclear fuels.

4. Texture plays an important role in reorientation of hydrides in Zr-2.5Nb pressure tubes and Zircaloy fuel cladding. Unusually low threshold stress for hydride reorientation reported for some Zr-2.5Nb pressure tube specimens is not applicable to commercial spent nuclear fuel cladding fabricated from Zircaloys because the texture of the pressure-tube specimens is significantly different from that of commercial spent nuclear fuel cladding. However, hydride reorientation can occur under repository conditions in PWR spent nuclear fuel cladding with burnups higher than ≈30 MWd/kgU, especially if peak cladding temperature exceeds ≈330°C.

5. Even if hydride reorientation occurs in a limited fraction of PWR spent fuel cladding discharged after burnups higher than ≈30 MWd/kgU, accompanying stress-rupture failure in the hydride-reoriented cladding is not likely to occur because the threshold stress for failure of irradiated and hydride-reoriented spent fuel cladding is significantly higher than the stress due to the internal pressure of the fuel rod. However, this conclusion is based on the results of a single experiment. The results were obtained for PWR fuel rods with a burnup of ≈30 MWd/kgU and are applicable to commercial spent nuclear fuel cladding under the repository conditions. However, the results should not be extended to fuels irradiated to higher burnups, especially for burnups higher than ≈55 MWd/kgU.

This document may be affected by technical product information that requires confirmation. Any changes to the document that may occur as a result of completing the confirmation activities will be reflected in subsequent revisions. The status of the input information quality may be confirmed by review of the Document Input reference System database,

8. INPUTS AND REFERENCES

8.1 DOCUMENTS CITED

Adamson, R.B. and Bell, W.L. 1985. "Effects of Neutron Irradiation and Oxygen Content on the Microstructure and Mechanical Properties of Materials." *Microstructure and Mechanical Properties of Materials.* 237-246. West Midlands, United Kingdom: Engineering Materials Advisory Services. TIC: 247022.

Aitchison, I. and Davies, P.H. 1993. "Role of Microsegregation in Fracture of Cold-Worked Zr-2.5Nb Pressure Tubes." Journal of Nuclear Materials, 203, 206-220. Amsterdam, The Netherlands: Elsevier Science. TIC: 246433.

Bai, J.B.; Ji, N.; Gilbon, D.; Prioul, C.; and Francois, D. 1994. "Hydride Embrittlement in Zircaloy-4 Plate: Part II. Interaction Between the Tensile Stress and the Hydride Morphology." *Metallurgical and Materials Transaction A, 25A*, (6), 1199-1208. Warrendale, Pennsylvania: The Minerals, Metals & Materials Society. TIC: 243932.

Chan, K.S. 1996. "A Micromechanical Model for Predicting Hydride Embrittlement in Nuclear Fuel Cladding Material." *Journal of Nuclear Materials, 227*, 220-236. Amsterdam, The Netherlands: Elsevier Science B.V. TIC: 237164.

Cheadle, B.A.; Coleman, C.E.; and Ambler, J.F.R. 1987. "Prevention of Delayed Hydride Cracking in Zirconium Alloys." *Zirconium in the Nuclear Industry, Seventh International Symposium Sponsored by ASTM Committee B-10 on Reactive and Refractory Metals, Strasbourg, France, 24-27, June 1985.* ASTM STP 939. 224-240. Philadelphia, Pennsylvania: American Society for Testing and Materials. TIC: 246152.

Chow, C.K. and Simpson, L.A. 1986. "Anlaysis of Unstable Fracture of a Reactor Pressure Tube Using Fracture Toughness Mapping." *Case Histories Involving Fatigue and Fracture Mechanics. ASTM STP 918,* 78-101. Philadelphia, Pennsylvania: American Society for Testing and Materials. TIC: 246151.

Chow, C.K.; Coleman, C.E.; Hobson, R.R.; Davies, P.H.; Griffiths, M.; and Choube 1991. "Fracture Toughness of Irradiated Zr-2.5Nb Pressure Tubes from CANDU Reactors." *Zirconium in the Nuclear Industry, 9th International Symposium, Kobe, Japan, November 5-8, 1990.* Eucken, C.M. and Garde, A.M., eds. *ASTM-STP-1132,* 246-275. Philadelphia, Pennsylvania: American Society for Testing and Materials. TIC: 246113.

Chung, H.M. 1987. "Phase Transformations in Neutron-Irradiated Zircaloys." *Radiation-Induced Changes in Microstucture: 13th International Symposium,* Garner, F.A.; Packan, N.H. and Kumar, A.S., eds. *(Part I), ASTM STP 955,* 676-699. Philadelphia, Pennsylvania: American Society for Testing and Materials. TIC: 246150.

Chung, H.M. and Yaggee, F.L. 1984. *Characteristics of Brittle-Type Fracture of High-Burnup Fuel Cladding Under Internal Gas-Pressurization Loading. Volume 1 Materials Science and Technology Division Light-Water-Reactor Safety Research Program: Quarterly Progress Report January-March 1983.* NUREG/CR-3689. Washington, D.C.: U.S. Nuclear Regulatory Commission. TIC: 246236.

Chung, H.M.; Yaggee, F.L.; and Kassner, T.F. 1987. "Fracture Behavior and Microstructural Characteristics of Irradiated Zircaloy Cladding." *Zirconium in the Nuclear Industry, Seventh International Symposium Sponsored by ASTM Committee B-10 on Reactive and Refractory Metals, Strasbourg, France, 24-27 June 1985.* Adamson, R.B. and Van Swam, L.F.P., eds. pp. 775-801. Philadelphia, Pennsylvania: American Society for Testing and Materials. TIC: 238255.

Coleman, C.E. 1982. "Effect of Texture on Hydride Reorientation and Delayed Hydrogen Cracking in Cold-Worked Zr-2.5Nb." *Zirconium in the Nuclear Industry: Fifth Conference. ASTM STP 754,* 393-411. Philadelphia, Pennsylvania: American Society for Testing and Materials. Library. Tracking Number 1274.

Coleman, C.E.; Cheadle, B.A.; Causey, A.R.; Chow, P.C.K.; Davies, P.H.; McManus, M.D.; Rodgers D.K.; Sagat, S.; and van Drunen, G. 1989. "Evaluation of Zircaloy-2 Pressure Tubes from NPD." *Zirconium in the Nuclear Industry: Eighth International Symposium, held 19-23 June 1988 at San Diego, California. ASTM STP 1023,* 35-49. Philadelphia, Pennsylvania: American Society for Testing and Materials. TIC: 241414.

CRWMS M&O 1998. *Waste Form Degradation and Radionuclide Mobilization Preliminary TSPA-VA Section (2.7).* B00000000-01717-2200-00199. Las Vegas, Nevada: CRWMS M&O. ACC: MOL.19980605.0187.

CRWMS M&O 1999a. *Classification of the MGR Uncanistered Spent Nuclear Fuel Disposal Container System.* ANL-UDC-SE-000001 REV 00. Las Vegas, Nevada: CRWMS M&O. ACC: MOL.19990928.0216.

CRWMS M&O 1999b. *1101213FM3 Waste Form Analyses & Models - PMR.* Activity Evaluation, December 14, 1999. Las Vegas, Nevada: CRWMS M&O. ACC: MOL.19991217.0048.

CRWMS M&O 2000a. *Waste Package Materials Department Analysis and Modeling Reports Supporting the Waste Form PMR.* TDP-EBS-MD-000005 REV 01 . Las Vegas, Nevada: CRWMS M&O. ACC: MOL.20000202.0173.

CRWMS M&O 2000b. *Repository Safety Strategy: Plan to Prepare the Postclosure Safety Case to Support Yucca Mountain Site Recommendation and Licensing Considerations.* TDR-WIS-RL-000001 REV 03. Las Vegas, Nevada: CRWMS M&O. ACC: MOL.20000119.0189.

Davies, P.H. and Stearns, C.P. 1986. "Fracture Toughness Testing of Zircaloy-2 Pressure Tube Material with Radial Hydrides Using Direct-Current Potential Drop." *Fracture Mechanics: Seventeenth Volume.* ASTM STP 905. 379-400. Philadelphia, Pennsylvania: American Society for Testing and Materials. TIC: 246153.

DOE (U.S. Department of Energy) 2000. *Quality Assurance Requirements and Description.* DOE/RW-0333P, Rev. 9. Washington, D.C.: U.S. Department of Energy, Office of Civilian Radioactive Waste Management. ACC: MOL.19991028.0012.

Efsing, P. and Pettersson, K. 1996. "The Influence of Temperature and Yield Strength on Delayed Hydride Cracking in Hydrided Zircaloy-2." *Zirconium in the Nuclear Industry: 11th International Symposium, ASTM STP 1295,* 394-404. West Conshohocken, Pennsylvania: American Society for Testing and Materials. TIC: 244499.

Einziger, R.E. and Kohli, R. 1984. "Low-Temperature Rupture Behavior of Zircaloy-Clad Pressurized Water Reactor Spent Fuel Rods Under Dry Storage Conditions." *Nuclear Technology, 67* (1), 107-123. Hinsdale, Illinois: American Nuclear Society. TIC: 216868.

Garde, A.M. 1989. "Effects of Irradiation and Hydriding on the Mechanical Properties of Zircaloy-4 at High Fluence." *Zirconium in the Nuclear Industry, 8th International Symposium.* Van Swam, L.F.P. and Eucken, C.M., eds. *ASTM-STP-1023,* 548-569. Philadelphia, Pennsylvania: American Society for Testing and Materials. TIC: 241414.

Garde, A.M.; Smith, G.P.; and Pirek, R.C. 1996. "Effects of Hydride Precipitate Localization and Neutron Fluence on the Ductility of Irradiated Zircaloy-4." ASTM-STP-1295 *Zirconium in the Nuclear Industry: 11th International Symposium.* Bradley, E.R. and Sabol, G.P., eds. pp. 407-430. Philadelphia, Pennsylvania: American Society of Testing and Materials. TIC: 244499.

Grigoriev, V. and Josefsson, B. 1998. "On the Mechanism of Zircaloy Cladding Axial Splits." *Journal of Nuclear Materials, 257,* 99-107. Amsterdam, The Netherlands: Elsevier Science B.V. TIC: 243432.

Guedeney, P.; Trotabas, M.; Boschiero, M.; Forat, C.; and Blanpain, P. 1991. "FRAGEMA Fuel Rod Behaviour Characterization at High Burnup." *Proceedings of the International Topical Meeting on LWR Fuel Performance, Fuel for the 90's, April 21-24, 1991, Avignon-France.* p. 627-638. LaGrange Park, Illinois: American Nuclear Society . TIC: 243519.

Hardie, D. and Shanahan, M.W. 1975. "Stress Reorientation of Hydrides in Zirconium-2.5% Niobium." *Journal of Nuclear Materials, 55,* 1-13. Amsterdam, The Netherland: North-Holland. TIC: 246261.

Henningson, P.J. 1998. *Cladding Integrity Under Long Term Disposal.* 51-1267509-00. Lynchburg, Virginia: Framatome Technologies. ACC: MOL.19990310.0103.

Leger, M.; Moan, G.D.; Wallace, A.C.; and Watson, N.J. 1989. "Growth, Fracture, and Nondestructive Evaluation of Hydride Blisters in Zr-2.5 Nb Pressure Tubes." *Zirconium in the Nuclear Industry, Eighth International Symposium held 19-23 June 1988 at San Diego, California.* Van Swam, L.F.P. and Eucken, C.M., eds. Pages 50-65. Philadelphia, Pennsylvania: American Society for Testing and Materials. TIC: 241414

Lemoine, F.; Cadarache, C.E.; M. Balourdet; and C.E. Cadarache 1997. "RIA Related Analytical Studies and Separate Effect Tests." *Proceedings of the 1997 International Topical Meeting on Light Water Reactor Fuel Performance, Portland, Oregon, March 2-6, 1997.* 693-703. La Grange Park, Illinois: American Nuclear Society. TIC: 232556.

Marshall, R.P. 1967. "Influence of Fabrication History on Stress-Oriented Hydrides in Zircaloy Tubing." *Journal of Nuclear Materials, 24,* 34-48. Amsterdam, The Netherlands: Elsevier Science, B.V. TIC: 246124.

McMinn, A.; Darby, E.C.; and Schofield, J.S. 2000. "The Terminal Solid Solubility of Hydrogen in Zirconium Alloys." *Zirconium in the Nuclear Industry: Twelfth International Symposium, Toronto, Canada, 15-18 June 1998.* Sabol, G.P. and Moan, G.D., eds. Pages 173-195. West Conshohocken, Pennsylvania: American Society for Testing and Materials. TIC: 247102.

Meyer, R.O.; McCardell, R.K.; Chung, H.M.; Diamond, D.J.; and Scott, H.H. 1996. "A Regulatory Assessment of Test Data for Reactivity-Initiated Accidents." *Nuclear Safety, 37,* (4), 271-288. Oak Ridge, Tennessee: Office of Scientific and Technical Information. TIC: 246287.

Moan, G.D.; Coleman, C.E.; Price, E.G.; Rogers, D.K.; and Sagat, S. 1990. "Leak-Before-Break in the Pressure Tubes of CANDU Reactors." *The International Journal of Pressure Vessels and Piping, 43,* 1-21. New York, New York: Elsevier Science Publishers. TIC: 246246.

Newman, L.W. 1986. *The Hot Cell Examination of Oconee 1 Fuel Rods After Five Cycles of Irradiation.* DOE/ET/34212-50. Lynchburg, Virginia: Babcock and Wilcox. TIC: 246679.

Onchi, T.; Kayano, H.; and Higashiguchi, Y. 1980. "The Inhomogeneous Deformation Behaviour of Neutron Irradiated Zircaloy-2." *Journal of Nuclear Materials,* 88, 226-235. Amsterdam, The Netherlands: Elsevier Science. TIC: 246438.

Onchi, T.; Kayano, H.; and Higashiguchi, Y. 1983. "The Inhomogeneous Plastic Deformation and its Relevance to Iodine Stress Corrosion Cracking Susceptibility in Irradiated Zircaloy-2 Tubing." *Journal of Nuclear Material.* 116, 211-218. Amsterdam, The Netherlands: Elsevier Science Publishers. TIC: 246318.

Papin, J.; Balourdet, M.; Lemoine, F.; Lamare, F.; Frizonnet, J.M.; and Schmitz, F. 1996. "French Studies on High-Burnup Fuel Transient Behavior Under RIA Conditions." *Nuclear Safety, 37,* (4), 289-327. Oak Ridge, Tennessee: Office of Scientific and Technical Information. TIC: 246288.

Peehs, M. and Fleisch, J. 1986. "LWR Spent Fuel Storage Behaviour." *Journal of Nuclear Materials, 137,* (3), 190-202. Amsterdam, The Netherlands: North-Holland Publishing Company. TIC: 235595.

Pescatore, C.; Cowgill, M.G.; and Sullivan, T.M. 1990. *Zircaloy Cladding Performance under Spent Fuel Disposal Conditions Progress Report May 1 - October 31, 1989.* BNL 52235. Upton, New York: Brookhaven National Laboratory. ACC: NNA.19900710.0055.

Puls, M.A.; Simpson, L.A.; and Dutton, R. 1982. "Hydride-Induced Crack Growth in Zirconium Alloys." *Fracture Problems and Solutions in the Energy Industry: Proceedings of the Fifth Canadian Fracture Conference, Winnipeg, Canada, 3-4 September 1981.* 13-25. Oxford, Great Britain: Pergamon Press. TIC: 246648.

Rothman, A.J. 1984. *Potential Corrosion and Degradation Mechanisms of Zircaloy Cladding on Spent Nuclear Fuel in a Tuff Repository.* UCID-20172. Livermore, California: Lawrence Livermore National Laboratory. ACC: NNA.19870903.0039.

S. Cohen & Associates 1999. Effectiveness of Fuel Rod Cladding as an Engineered Barrier in the Yucca Mountain Repository. McLean, Virginia: S. Cohen & Associates. TIC: 246541.

Shi, S.Q. and Puls, M.P. 1996. "Advances in the Theory of Delayed Hydride Cracking in Zirconium Alloys." *Hydrogen Effects in Materials: Proceedings of the Fifth International Conference on the Effect of Hydrogen on the Behavior of Materials Sponsored by the Structural Materials Division (SMD).* 611-621. Warrendale, Pennsylvania: Minerals, Metals & Materials Society. TIC: 239793.

Simpson, L.A. and Cann, C.D. 1979. "Fracture Toughness of Zirconium Hydride and its Influence on the Crack Resistance of Zirconium Alloys." *Journal of Nuclear Materials, 87,* 303-316. Amsterdam, The Netherlands: Elsevier Science Publishers. TIC: 246317.

Simpson, L.A. and Puls, M.P. 1979. "The Effects of Stress, Temperature, and Hydrogen Content on Hydride-Induced Crack Growth in Zr-2.5%Nb." *Metallurgical Transactions A, 10A,* 1093-1105. Materials Park, Ohio: American Society for Metals International. TIC: 246145.

Smith, G.P., Jr.; Pirek, R.C.; Freeburn, H.R.; and Schrire, D. 1994. *The Evaluation and Demonstration of Methods for Improved Nuclear Fuel Utilization.* DOE/ET/34013-15. Washington, D.C.: U.S. Department of Energy. TIC: 245407.

Snowden, K.U. and Veevers, K. 1973. "Radiation Hardening in Zircaloy-2." *Radiation Effects, 20,* (3), 169-174. New York, New York: Gordon and Breach Science. TIC: 246245.

Stout, R.B. 1989. *A Deformation and Thermodynamic Model for Hydride Precipitation Kinetics in Spent Fuel Cladding.* UCRL-100860 (Preprint). Livermore, California: Lawrence Livermore National Laboratory. ACC: NNA.19900419.0137.

Wallace, A.C.; Shek, G.K.; and Lepik, O.E. 1989. "Effects of Hydride Morphology on Zr-2.5Nb Fracture Toughness." *Zirconium in the Nuclear Industry: Eighth International Symposium, held 19-23 June 1988 at San Diego, California. ASTM STP 1023,* 66-88. Philadelphia, Pennsylvania: American Society for Testing and Materials. TIC: 241414.

Westlake, D.G. 1968. "The Habit Planes of Zirconium Hydride in Zirconium and Zircaloy." *Journal of Nuclear Materials, 26,* 208-216. Amsterdam, The Netherland: North Holland. TIC: 246247.

Yang, R.L.; Ozer, O.; and Klepfer, H.H. 1991. "Fuel Performance Evaluation for EPRI Program Planning." Volume 1 of *International Topical Meeting on LWR Fuel Performance, Avignon (France), April 21-24, 1991, Proceedings, Fuel for the 90's.* 258-271. La Grange Park, Illinois: American Nuclear Society. TIC: 243519.

Yuan, X.Q. and Tangri, K. 1982. "Metallographic Observations on the Developing Hydride Morphology at the Crack Tip During Hydrogen Induced Delayed Cracking in a Zr-2.5Nb Alloy." *Journal of Nuclear Materials, 105,* 310-317. Amsterdam, The Netherlands: North Holland. TIC: 246250.

8.2 CODES, STANDARDS, REGULATIONS, AND PROCEDURES

AP-3.10Q, Rev. 2, ICN 0. *Analyses and Models.* Washington, D.C.: U.S. Department of Energy, Office of Civilian Radioactive Waste Management. ACC: MOL.20000217.0246.

AP-3.15Q, Rev. 0, ICN 2. *Managing Technical Product Inputs.* Washington, D.C.: U.S. Department of Energy, Office of Civilian Radioactive Waste Management. ACC: MOL.19991123.0068.

QAP-2-0, Rev. 5, ICN 1. *Conduct of Activities.* Las Vegas, Nevada: CRWMS M&O. ACC: MOL.19991109.0221.

QAP-2-3, Rev. 10. *Classification of Permanent Items.* Las Vegas, Nevada: CRWMS M&O. ACC: MOL.19990316.0006.